11-11-2014

A plausible mechanism, based upon SHORT-ROOT movement, for regulating the number of cortex cell layers in roots.

Shuang Wu
Department of Biology, University of Pennsylvania

Chin-Mei Lee
Department of Biology, University of Pennsylvania

Tomomi Hayashi
Department of Biology, University of Pennsylvania; Department of Biomedical Sciences, Thomas Jefferson University, Tomomi.Iwasaki-Hayashi@jefferson.edu

Simara Price
Department of Biology, University of Pennsylvania

Fanchon Divol
Centre de Coopération Internationale en Recherche Agronomique pour le Développement, UMR Amélioration Génétique et Adaptation des Plantes Cultivées (AGAP)

See next page for additional authors

Authors
Shuang Wu, Chin-Mei Lee, Tomomi Hayashi, Simara Price, Fanchon Divol, Sophia Henry, Germain Pauluzzi, Christophe Perin, and Kimberly L Gallagher

A plausible mechanism, based upon SHORT-ROOT movement, for regulating the number of cortex cell layers in roots

Shuang Wu[a], Chin-Mei Lee[a], Tomomi Hayashi[a,1], Simara Price[a], Fanchon Divol[b], Sophia Henry[b], Germain Pauluzzi[b], Christophe Perin[b], and Kimberly L. Gallagher[a,2]

[a]Department of Biology, University of Pennsylvania, Philadelphia, PA 19104; and [b]Centre de Coopération Internationale en Recherche Agronomique pour le Développement (CIRAD), UMR Amélioration Génétique et Adaptation des Plantes Cultivées (AGAP), F34398 Montpellier, France

Edited by G. Venugopala Reddy, University of California, Riverside, CA, and accepted by the Editorial Board September 25, 2014 (received for review April 23, 2014)

Formation of specialized cells and tissues at defined times and in specific positions is essential for the development of multicellular organisms. Often this developmental precision is achieved through intercellular signaling networks, which establish patterns of differential gene expression and ultimately the specification of distinct cell fates. Here we address the question of how the SHORT-ROOT (SHR) proteins from *Arabidopsis thaliana* (AtSHR), *Brachypodium distachyon* (BdSHR), and *Oryza sativa* (OsSHR1 and OsSHR2) function in patterning the root ground tissue. We find that all of the SHR proteins function as mobile signals in *A. thaliana* and all of the SHR homologs physically interact with the AtSHR binding protein, SCARECOW (SCR). Unlike AtSHR, movement of the SHR homologs was not limited to the endodermis. Instead, the SHR proteins moved multiple cell layers and determined the number of cortex, not endodermal, cell layers formed in the root. Our results in *A. thaliana* are consistent with a mechanism by which the regulated movement of the SHR transcription factor determines the number of cortex cell layers produced in the roots of *B. distachyon* and *O. sativa*. These data also provide a new model for ground tissue patterning in *A. thaliana* in which the ability to form a functional endodermis is spatially limited independently of SHR.

SHORT-ROOT | root development | cellular patterning | SCARECROW | rice

The root of *Arabidopsis thaliana* is composed of distinct single cell layers that are concentrically arranged around a central core of largely vascular tissues, which, along with the pericycle, forms the stele. The ground tissue layers, endodermis plus cortex, directly surround the stele. The ground tissue of most, if not all, roots contains a single layer of endodermis, which forms a water-impermeable barrier that protects the vascular tissues. To the outside of the endodermis is the cortex. The number of cortex cell layers differs between roots of different species, and in some cases, between roots (e.g., primary versus lateral) on the same plant. In *A. thaliana,* where root development has been extensively examined, the number of ground tissue layers in both primary and secondary roots is two, with a single endodermal and a single cortical cell layer (1). In contrast, the roots of both *Brachypodium distachyon* and *Oryza sativa* (rice) have a single layer of endodermis but multiple layers of cortex, with the number of cortex cell layers varying between root types (2, 3). For example, in the primary root of rice, there are five to six layers of cortex, but in some of the thin lateral roots, there may be only one layer of cortex. In all roots, it is thought that the number of endodermal cell layers is controlled through the conserved function and regulation of the SHR transcriptional network (4); however, it is not known how the number of cortex cell layers is adjusted. Here we show that controlled movement of SHORT-ROOT (SHR) in *A. thaliana* regulates the number of cortex cell layers independent of the number of endodermal cell layers. SHR movement may therefore represent a tunable mechanism for controlling the number of cortex cell layers in roots.

In *A. thaliana,* as in other dicots, the endodermis and cortex are clonally related cell layers that arise from the asymmetric periclinal cell divisions of a cortical endodermal daughter (CED) cell located at the tip of the root adjacent to the stele. Division of the CED is under the control of the SHR and the SCARECROW (SCR) transcription factors. The SHR protein is expressed in the stele and moves into the neighboring endodermis and CED cells where it activates the expression of the downstream transcription factor, SCR. In the CED, SHR and SCR together activate expression of a D-type cyclin (CYCD6;1), which triggers periclinal division of the CED (5–8). The CED cells of roots that lack SHR or SCR fail to divide periclinally and therefore form only a single layer of ground tissue. Roots that lack SHR fail to specify an endodermis, so the single ground tissue layer in *shr-2* null mutants has cortex cell identity. In contrast, roots that lack SCR form a chimeric ground tissue layer with aspects of both cortical and endodermal cell fates. These results show that SHR, independent of cell division, is required for endodermal cell fate.

The prevailing model for how a single layer of endodermis is formed in *A. thaliana* is that once SHR turns on the expression of SCR in the endodermis, SCR physically interacts with SHR and sequesters SHR in the nuclei of endodermal cells, preventing further movement into the cortex cell file (Fig. 1) (4). In addition to SCR, the JACKDAW (JKD) and MAGPIE (MGP) transcription factors may also play a role in limiting SHR movement, again through direct binding to the SHR protein (9). Because, outside of

Significance

In nature, nearly all plants have only a single layer of endodermis. The number of cortex cell layers often varies between species and between roots on the same plant. Here we show that the expression of conserved SHORT-ROOT (SHR) protein, in the context of the root of *Arabidopsis thaliana,* is responsible for determining the number of cortex cell layers and that the number of cell layers is a function of the extent of SHR movement. These results provide a plausible model for regulating the number of cortex cell layers in plant roots that relies upon controlled intercellular movement of the SHR transcription factor.

Author contributions: S.W., C.-M.L., C.P., and K.L.G. designed research; S.W., C.-M.L., T.H., S.P., F.D., S.H., G.P., C.P., and K.L.G. performed research; S.W., C.-M.L., S.P., C.P., and K.L.G. analyzed data; and S.W., C.-M.L., and K.L.G. wrote the paper.

The authors declare no conflict of interest.

This article is a PNAS Direct Submission. G.V.R. is a guest editor invited by the Editorial Board.

[1]Present address: Department of Biomedical Sciences, Thomas Jefferson University, Philadelphia, PA 19107.

[2]To whom correspondence should be addressed. Email: gallagkl@sas.upenn.edu.

This article contains supporting information online at www.pnas.org/lookup/suppl/doi:10.1073/pnas.1407371111/-/DCSupplemental.

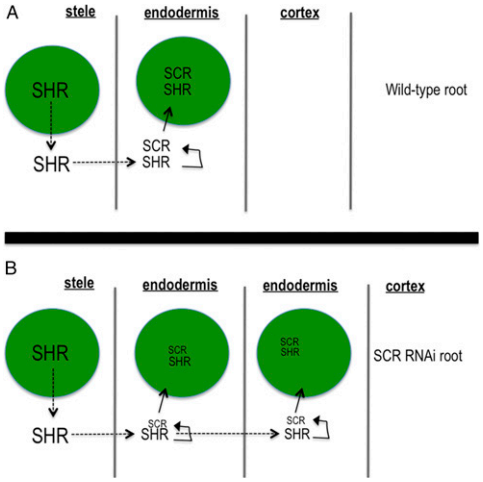

Fig. 1. Cartoon summarizing the prevailing model for ground tissue patterning proposed by Cui et al. (4). The green circles are nuclei. Dotted lines indicate protein movement. The size of the font is meant to indicate the amount of the protein. (*A*) The pathway for the formation of a normal root and (*B*) one in which SCR is reduced via RNAi.

the stele, SHR is thought to be both necessary and sufficient for endodermal cell specification, the physical interaction between SHR and SCR prevents the formation of additional endodermal cell layers by limiting SHR movement. This model is supported by the finding that the domain of SHR movement is increased in SCR knockdown lines (*SCR* RNAi; Fig. 1) and that increases in the extent of SHR movement lead to the formation of additional SCR-expressing cell layers, with SCR expression being used as a marker of endodermis (4). Also in support of this model is the finding that ectopic expression of SHR can cause cells to produce suberin, a waxy substance produced by the endodermis. Although JKD and MGP also affect the movement of SHR, they appear to affect the position of the endodermis but not the number of endodermal cell layers (9).

Because all plants have a single layer of endodermis in the mature root, and most plants contain homologs of both SHR and SCR, Cui et al. (4) tested whether the physical interaction between SHR and SCR is conserved in rice. They found that OsSHR1 interacted with both OsSCR1 and AtSCR in yeast. Based upon these findings, they proposed an elegant model in which the interaction between SHR and SCR represents an evolutionarily conserved mechanism that delimits SHR movement and thereby defines a single layer of endodermis (4). Although this mechanism for the specification of a single endodermis is often cited in the literature, the hypothesis has not been fully tested. In addition, this model provides no mechanism for the formation of extra cortex cell layers in roots like those of rice.

Here, using the SHR protein from *A. thaliana* and the homologous SHR proteins from two species of grasses, *Brachypodium distachyon* and *Oryza sativa,* we examined the function of SHR in the root of *A. thaliana*. All of the SHR homologs were able to move out of the stele into the ground tissue. The movement of the SHR proteins was dependent upon plasmodesmata (intercellular channels that connect plant cells) and conserved sequences within the GRAS domain of the SHR proteins. Interestingly, we found that although all of the SHR homologs interacted strongly with AtSCR (as well as AtMGP and AtJKD), their movement was not limited to a single layer of ground tissue, indicating that physical association between SHR and SCR is insufficient to restrict SHR movement within the endodermis. In addition, although all of the SHR proteins had the ability to restore endodermal specification in the *shr-2* mutants, none of them (including AtSHR) had the ability to specify more than one layer of functional endodermis. Instead, all extra cell layers produced by the expression of the SHR proteins adopted cortex cell characteristics. In contrast with previous findings (4), our results show that the ability of SHR to specify endodermis is spatially limited to the cell layer immediately outside of the stele. Therefore, our data significantly revise the previous established model for the regulation of ground tissue patterning (Fig. 1) and suggest a credible mechanism by which the regulated movement of SHR controls the number of cortex cell layers produced in roots of different species.

Results

The SHR Homologs Are Mobile and Move Beyond the Endodermis. Although a single endodermis seems to be the rule in normal root development, multiple layers of cortex are common in many plant species, including rice and *B. distachyon* (Fig. S1) (2, 3). When expressed as a YFP fusion under the *AtSHR* promoter in either wild-type or in *shr-2* mutant roots, OsSHR1 (LOC_Os7g39820), OsSHR2 (LOC_Os3g31880), and BdSHR (LOC100830802) were detected as YFP fusions in multiple cell layers beyond the stele forming a protein gradient with the highest levels directly outside of the stele (Fig. 2 *A* and *B*) These results indicate that all of the SHR proteins are mobile. Similar to AtSHR, the YFP-tagged SHR homologs all showed both nuclear and cytoplasmic localization in the stele (Fig. 2 *A* and *C*); outside of the stele the protein localization was restricted to the nucleus (Fig. 2*A*), indicating that similar mechanisms control the subcellular localization of the *A. thaliana* and the grass SHR proteins.

To determine whether the mechanisms promoting the intercellular movement of OsSHR1, OsSHR2, BdSHR, and AtSHR are similar, we examined the role of a conserved threonine (T289) in protein transport. In AtSHR, mutation of T289 to alanine (A), in the VHIID domain of the protein, inhibits nuclear localization and intercellular movement of AtSHR (4). We converted the conserved threonine to alanine in OsSHR1, OsSHR2, and BdSHR and found that as in AtSHR, the conserved threonine is required for nuclear localization and movement of all three of the SHR homologs

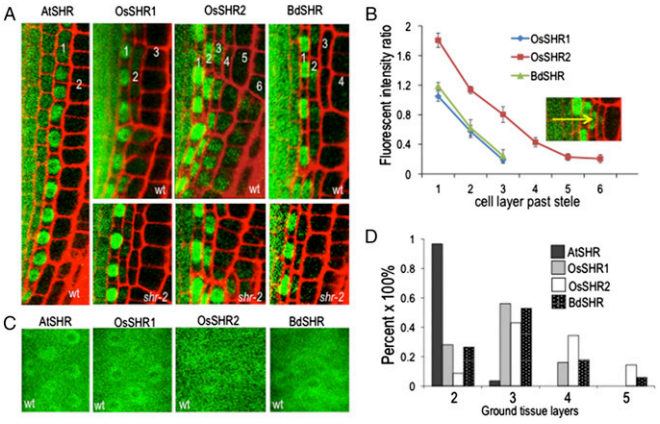

Fig. 2. The monocot SHR proteins move beyond the endodermis in *A thaliana* roots. (*A*) Confocal images of the SHR homologs expressed as YFP fusions under the *SHR* promoter in both wild-type (*A*, as labeled, *B*–*D*) and in *shr-2* (*A*, as labeled) roots. The numbers represent the ground tissue layers relative to the stele, which are quantified in *D*. (*B*) The SHR homologs as YFP fusions formed a protein gradient, with the highest levels in the cell layer directly outside of the stele. The *Inset* is a representative image from OsSHR2-YFP, and the arrow shows the direction of the gradient. The relative fluorescence intensity was quantified using the fluorescence intensity of each ground tissue layer against that in stele (n = 8 roots, 96 cells for each SHR homolog). (*C*) Confocal image showing the YFP-tagged SHR homologs localized to both the nucleus and cytoplasm of stele cell. (*D*) Quantification of additional ground tissue layers caused by the expression of SHR homologs (n = 3 replicates, 36 roots for each SHR homolog).

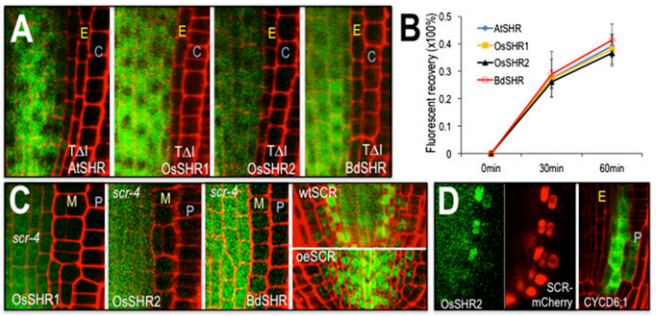

Fig. 3. The SHR proteins have similar requirements for localization and movement. (*A*) Mutation of a conserved threonine (residue 289 in AtSHR, 345 in OsSHR1, 352 in OsSHR2, and 354 in BdSHR) in the VHIID domains of the SHR proteins inhibits nuclear localization and intercellular movement. C, cortex; E, endodermis. Full root tip images are in Fig. S2. (*B*) Quantification of fluorescence recovery after photobleaching (FRAP) showed that the kinetics of protein movement between the stele and the first ground tissue is comparable among all SHR homologs [$n = 3$ replicates, 9 roots and 35–132 cells for each SHR homolog; assays were done in wild type (WT)]. (*C*) The *scr-4* mutation is epistatic to the effects of expression of the SHR homologs. M, mutant cell layer; P, epidermis. The first three panels show transgene expression from the SHR promoter in the scr-4 (null) background. The last two panels show OsSHR2-YFP in a WT root and a root overexpressing (oe) AtSCR-mTFP from the SHR promoter. (*D*) Expression of OsSHR2 from the SHR promoter (*Left and Middle*) drives expression of the SCR:mCherry marker and expression of CYCD6;1:erGFP (*Right*), which is visualized without the OsSHR2-YFP signal.

(Fig. 3*A* and Fig. S2). To determine whether the kinetics of protein movement are similar for the SHR proteins, we measured the fluorescent recovery of the BdSHR-YFP, OsSHR1-YFP, and OsSHR2-YFP proteins after photobleaching of the YFP signal in the inner ground tissue layers. The kinetics of recovery were similar for all of the SHR proteins (Fig. 3*B* and Fig. S3), indicating that these proteins traffic by a similar, if not the same, pathway.

Previously, we showed that the intercellular movement of AtSHR occurs via plasmodesmata (PD) (10). PD-dependent movement of AtSHR was demonstrated using a semidominant inducible allele of callose synthase (*icals3m*) that deposits callose around the PD in response to estradiol treatment. The accumulation of callose around the PD decreases the PD aperture and movement of the SHR protein from the stele into the endodermis. Induction of the *icals3m* transgene (expressed in the stele from the WOODENLEG promoter) reliably blocked movement of the OsSHR1 and OsSHR2 proteins from the stele into the ground tissue layers (Fig. S4). Collectively, these results indicate a conserved mechanism for intercellular protein movement among the different SHR homologs.

SHR Homologs Interact With SCR, MGP, and JKD Proteins and Rely on SCR Expression for Movement and Function. In *A. thaliana,* generation of extra ground tissue layers by ectopic expression of AtSHR is dependent upon SCR. In the absence of SCR, extra cell layers do not form (7). To test whether the phenotype generated by expression of the SHR homologs in *A. thaliana* is also dependent upon SCR, we crossed the transgenic lines expressing BdSHR-YFP, OsSHR1-YFP, and OsSHR2-YFP into a *scr-4* (null) mutant background. In all cases, the *scr-4* mutation was largely epistatic to the effects of the expression of the SHR homologs on root patterning (Fig. 3*C*). Expression of BdSHR and OsSHR1 in *scr-4* marginally decreased the time until middle cortex formation (from day 7 to day 4), which normally forms precociously in *scr-4* mutants (11); however, there were no other changes in the *scr-4* phenotype. Interestingly, nuclear localization and movement of BdSHR-YFP, OsSHR1-YFP, and OsSHR2-YFP appeared decreased in the *scr-4* background, which is similar to what we previously reported for AtSHR movement (12, 13), indicating a similar mechanism for the nuclear localization and intercellular movement of the SHR proteins.

The heart of the SCR-SHR sequestration model is that interaction between SCR and SHR in the presumptive endodermis limits SHR movement and this restricts the root to a single layer of endodermis (Fig. 1) (4). Because BdSHR, OsSHR1 and OsSHR2 all moved beyond the endodermis and their movement and localization is dependent upon SCR, we tested whether these homologs could directly interact with AtSCR using yeast two-hybrid and bimolecular fluorescence complementation (BiFC) assays. Based upon yeast growth assays, all of the SHR homologs interacted with AtSCR, as well as with MGP and JKD, which have been shown to interact with AtSHR (Fig. 4*A* and Fig. S5) (9). Based upon their growth on selective media, all of the homologs showed similar levels of interaction with AtSCR as did AtSHR. Quantitative BiFC (Fig. S5), as measured in *A. thaliana* protoplast, showed no significant difference in interaction between any of the SHR proteins and AtSCR. In yeast, using normalized levels of beta-galactosidase activity, of all of the SHR proteins (including AtSHR), BdSHR showed the strongest interaction with AtSCR (Fig. 4*B*). These results show that the increased movement of BdSHR, OsSHR1, or OsSHR2 compared with AtSHR cannot be explained simply by an inability to interact with AtSCR, nor do the strengths of interactions with AtSCR correlate with the extent of movement. Because rice has two SCR proteins, OsSCR1 and OsSCR2, we tested for interaction between the OsSHR proteins with OsSCR. As shown in Fig. 4, both OsSHR1 and OsSHR2 interacted with OsSCR1 and OsSCR2.

To test further the role of AtSCR in the localization and movement of the monocot SHR proteins, we examined the

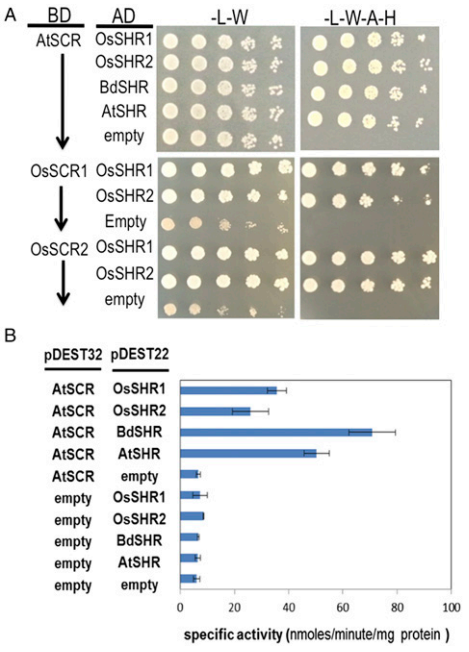

Fig. 4. The SHR homologs interact with SCR. (*A*) Fivefold serial dilutions of diploid yeast expressing AtSCR, OsSCR1, or OsSCR2 as bait with the SHR prey proteins (as labeled) grown on selective medium. Medium lacking adenine and histidine was used to select for interaction between the bait and prey proteins. AD, activation domain vector (prey); BD, binding domain vector (bait). BiFC results are shown in Fig. S5*A*. (*B*) Quantitative beta-galactosidase assays showing the specific activity of the beta-galactosidase enzyme induced by the interaction of the bait and prey proteins. The interacting proteins are as labeled. Assays were done in diploid yeast and normalized to total protein.

localization and movement of OsSHR2 in roots that ectopically express AtSCR from the SHR promoter (Fig. 3*C*). As previously reported, expression of SCR-TFP in the stele (from the AtSHR promoter) results in the nuclear localization of AtSHR-GFP in the stele; the AtSHR-GFP does not move out of the stele, and the endodermis is not formed. When SHR:SCR-TFP was crossed into plants expressing OsSHR2, there was a dramatic increase in the nuclear localization of OsSHR2 in stele cells. However, there were no effects on the movement of OsSHR2 out of the stele or on the production of ground tissue layers. These results indicate the AtSCR promotes the nuclear localization of OsSHR protein but cannot block its movement.

The SHR Homolog Can Partially Substitute for AtSHR. The roots of *shr-2* mutants are significantly shorter than wild type; they have a smaller meristem (based both upon the length of the meristem and cell number) and lack an endodermis. To determine whether the monocot SHR proteins could substitute for AtSHR, OsSHR1, OsSHR2, or BdSHR was crossed into the *shr-2* mutant background and both root growth and patterning were assessed (Fig. S6). Expression of either OsSHR1or BdSHR in *shr-2* was able to fully rescue root growth and meristem size; OsSHR2 provided a partial rescue of the *shr-2* phenotype with restoration of root growth to nearly wild-type levels (Fig. S6*D*) and a 48.6% rescue in the size of the meristem (Fig. S6*E*). Although the monocot SHR proteins were able to restore growth of *shr-2* roots, all of the SHR homologs produced an "over-rescue" phenotype with the formation of multiple ground tissue layers (Fig. 2*A*). These results indicate that in most cases, the SHR homologs can functionally substitute for AtSHR.

In both wild-type and *shr-2* mutants, expression of the homologous *SHR* transgenes in *A. thaliana* resulted in the formation of additional ground tissue layers with OsSHR2 showing the greatest potential for inducing extra cell layers (Fig. 2 *A* and *D* and Fig. S1 *C*–*F*). In wild-type *A. thaliana* roots, movement of SHR into the cortical endodermal initial (CEI) and the CED cell up-regulates SCR, which, together with SHR, turns on *CYCLIND6;1* (*CYCD6;1*) (8). In the CED cells, expression of *CYCD6;1* triggers the asymmetric periclinal cell division that creates the separate endodermal and cortical cell layers. Consistent with an induction of periclinal cell divisions in the generation of extra cell layers in the roots expressing the rice and *B. distachyon* SHRs, SCR is expressed beyond the endodermis (Fig. 3*D*) and CYCD6;1 is expressed not only in the CEI and the CED cells but also in the cortical cell lineages. In 6-d-old roots, expression of *CYCD6;1* was particularly enriched in the outer cortex cell layers. Occasionally, expression was also seen in the epidermis (2 out of 10 roots) and the endodermis (1 out of 10 roots) (Fig. S7) (8, 12, 14, 15). These results are consistent with the ectopic movement of the OsSHR1, OsSHR2, and BdSHR proteins inducing SCR and CYCD6;1, which leads to ectopic periclinal cell divisions in the cortex.

The Monocot SHRs Specify a Single Layer of Endodermis and Multiple Layers of Cortex. To determine the identity of the additional cell layers created by the expression of OsSHR1, OsSHR2, or BdSHR, we examined cell-type specific markers of the endodermis (ENDODERMIS7:Histone2B:mCherry, referred to here as EN7-HC) and cortex (CORTEX2:Histone2B:mCherry, referred to here as pCO2-HC) (16) in wild-type roots expressing the monocot SHR proteins. We found an inverse correlation between expression of the EN7-HC and the CO_2-HC markers, with cells near the root tip transiently expressing EN7-HC and cells in the distal region of the meristem expressing CO_2-HC (Fig. 5*A* and Fig. S8 *A*–*F*). To better understand the determination of cell fate within the extra ground tissues, we quantified the fluorescence intensity of the EN7-HC and CO_2-HC makers in the first extra cell layer and the results were normalized to the endodermis or the cortex. We found that in the first additional cell layer, EN7-HC expression was highest adjacent to the quiescent center (QC) and then decreased dramatically in the shootward direction (Fig. 5*B*). The level of EN7-HC was reduced by 80% in cells separated from the CEI by four rounds of anticlinal (transit amplifying) cell divisions. In this region of the root where EN7-HC levels dropped, CO_2-HC expression was initiated (Fig. 5*B*). The intensity of CO_2-HC within the first extra cell layer increased sevenfold after an additional five rounds of anticlinal cell division, indicating that the additional ground tissue layers that are not in direct contact with the stele transiently express EN7-HC, but then quickly adopt a cortex cell identity as they are displaced into the distal meristem (shootward) via transit amplifying cell divisions.

To further verify the identity of the extra ground tissues layers, we crossed a functional marker of cell identity, the PIN2:PIN2-GFP (PIN-FORMED 2) auxin efflux carrier into a line expressing OsSHR2. In wild-type *A. thaliana* roots, PIN2 is absent from the endodermis and is expressed in the cortex and the epidermis (Fig. 5*C*). In the epidermis, PIN2 localizes to the basal region (the shootward side) of cells, while it is restricted to the apical end (rootward side) of cells in the cortex (17). In roots expressing OsSHR2, which had the most dramatic effect on root patterning, the additional cell layers all expressed rootward-localized PIN2 (Fig. 5 *D* and *E*); this is similar to the region of the root meristem in which expression of pCO2-HC was initiated. These results indicate that the ectopic cell layers generated by the expression and movement of the monocot SHRs adopt a cortex cell fate rather than an endodermal or an epidermal cell fate.

One of the distinguishing features of the endodermis is the formation of lignin-rich Casparian strips that encircle each cell in the layer. In the *A. thaliana* root, the endodermis is the only cell layer to form Casparian strips (i.e., there is no exodermis), so in wild-type roots, there is a single layer of lignified cells that surrounds the stele. In the roots expressing the monocot SHR proteins, we also detected a single lignified cell layer surrounding the

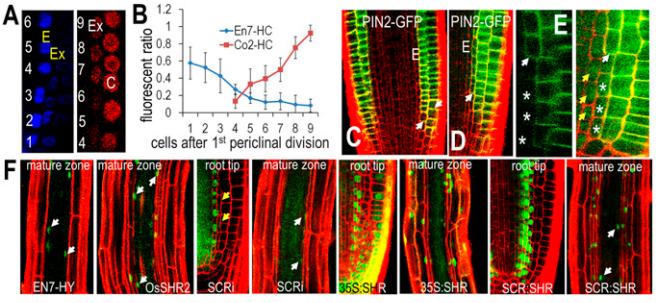

Fig. 5. The extra ground tissue cell layers induced by the SHR homologs have a cortical cell identity. (*A*) Representative images of expression of EN7-HC (pseudocolored in blue) and CO_2-HC (in red) that is quantified in *B*. C, cortex; E, endodermis; Ex, the extra cell layer that was measured in the calculation of the fluorescence ratio shown in *B*. The numbers show the location of cells relative to the first divided initial cell at root tip. (*B*) Quantification of the fluorescence ratio between Ex and E or Ex and C as labeled ($n = 8$ roots, 41–68 cells for each marker). Co2-HC, pCo2-H2B-mCherry; En7-HC, pEN7-H2B-mCherry. (*C*) *PIN2:PIN2-GFP* expression in wild type. PI staining (red) was used to visualize cell boundaries. The arrows point to the cortex cells that start to express PIN2-GFP. E, endodermis. (*D*) PIN2:PIN2-GFP in roots expressing OsSHR2. Cell layers were shown by PI staining in red. The arrow points to the additional cell layer that starts to express PIN2-GFP. (*E*) Magnified images of the meristem expressing PIN2:PIN2-GFP in OsSHR2-expressing roots. *Left* shows just PIN-GFP; whereas *Right* also shows OsSHR2-YFP. The white arrows point to cells that first start to express PIN2-GFP. Yellow arrows point to the nuclear localization of OsSHR2 in the presumptive endodermis. The asterisks mark the same cells in *Left* and *Right*. (*F*) PI is excluded from the stele and a single ground tissue layer (the endodermis) in all genotypes (as labeled). The white arrows point to nuclei in the endodermis.

PLANT BIOLOGY

stele (Fig. S8 *G–J*), indicating the presence of a single layer of endodermis (18). Similar to the epithelium in animals, the endodermis establishes a paracellular (apoplastic) diffusion barrier in plants (19). Consistent with an ability to block diffusion, Naseer et al. recently showed that functional Casparian strips (and therefore a functional endodermis) blocks the flux of propidium iodide (PI) solution into the stele so that only the epidermis and cortex are stained with PI in the mature zone of an *A. thaliana* root; the endodermis and stele cells are unstained (18). In the wild-type roots expressing OsSHR1, OsSHR2, or BdSHR, PI was excluded from the stele and a single cell layer of ground tissue immediately surrounding the stele. These results indicate that there is a single functional layer of endodermis regardless of the number of extra ground tissue layers in the root (Fig. 5*F*).

These results are consistent with the ability of the monocots SHRs to induce the formation of multiple layers of cortex in rice and brachypodium. In *A. thaliana,* AtSHR is required for the formation of a functional endodermis. Therefore, we tested whether OsSHR1, OsSHR2, or BdSHR could restore endodermal cell fate in the context of the *shr-2* roots. The expression of any of the SHR homologs in *shr-2* resulted in the exclusion of PI from the stele and a single cell layer of ground tissue immediately surrounding the stele, but not from any of the additional cell layers of ground tissue. (Fig. S8 *N–P*). Because *shr-2* mutants have no endodermis and cannot exclude PI (Fig. S8*M*), these results indicate that the SHR homologs have the ability to specify endodermis. However, in all roots examined, the ability to induce endodermis was spatially limited to the single cell layer adjacent to the stele. Thus, the expression of OsSHR1, OsSH2, or BdSHR does not alter the number of endodermal cell layers.

Ectopic Movement or Expression of AtSHR Does Not Result in the Formation of Additional Functional Endodermal Cell Layers. The results of our analyses with AtSHR and the homologs from rice and *B. distachyon* suggest that although the movement and regulation of these proteins are similar, the monocot SHR proteins (even in the presence of an increased domain of movement) have a spatially limited ability to specify endodermis. In the wild-type and the *shr-2* roots expressing BdSHR, OsSHR1, or OsSHR2, PI penetrated into the root and the extra cell layers surrounding the stele. However, PI did not penetrate the stele cells and was also restricted from a single ground tissue layer surrounding the stele, indicating that these proteins alone are not sufficient to induce the formation of endodermis (18). This is in contrast to the AtSHR, whose increased movement is thought to result in the formation of ectopic endodermis (7, 9, 16, 20). Expression of SHR is thought to be both necessary and sufficient for the induction of endodermal cell fate.

In Cui et al., the presence of extra endodermal layers was shown by the expression of SCR in the supernumerary layers (4). In Nakajima et al. (7), the formation of extra endodermal cell layers in roots expressing SHR from the SCR promoter (SCR:SHR) was shown by expression of SCR in the cells, as well as by the accumulation of suberin, which is associated with Casparian strips. However, no functional assays were performed to test for the presence of additional layers of endodermis in either the SCR RNAi (4) or the SCR:SHR lines. To determine whether ectopic movement or expression of AtSHR can produce a functional endodermis, we examine PI exclusion in SCR RNAi-, 35S:SHR-GFP–, and SCR:SHR-nlsGFP–expressing lines, all of which produce extra ground tissue. In SCR RNAi lines (4), we found that the supernumerary layers did not restrict PI movement, indicating that these roots do not form additional functional endodermal cell layers (Fig. 5*F*). Likewise, in roots constitutively expressing SHR (*35S:SHR-GFP*) or roots expressing SHR directly in the ground tissue (*SCR:SHR-nlsGFP*) (Fig. 5*F*) (6), the extra layers were not lignified (Fig. S8*K*) nor did they behave as a functional endodermis (Fig. S8*L*). These results suggest that AtSHR alone is not sufficient to induce a functional endodermis. In *A. thaliana* and likely in the roots of other plant species, we propose that an additional factor, perhaps derived from the stele, is required for SHR to specify a functional endodermis.

Discussion

In examining the movement capacity and function of the rice and *B. distachyon* homologs of AtSHR, we find compelling evidence for a conserved mechanism for SHR movement and ground tissue patterning. The movement of all of the SHR proteins was similar in terms of the kinetics of protein movement, the requirement for a conserved threonine in the VHIID domain of the protein, and a role for SCR in promoting nuclear localization of SHR and movement from the stele into the endodermis. With respect to protein function, expression of any one of the *B. distachyon* or *O. sativa* homologs of AtSHR was able to rescue endodermal cell fate in the *shr-2* mutant background. In addition, both BdSHR and OsSHR1 were able to complement defects in the meristem of the *shr-2* plants, as well as root growth. Unlike AtSHR, movement of the monocot SHRs was not limited to a single layer of ground tissue. The increased movement of the SHR proteins produced multiple layers of cortex cell. In no instances did we observe more than one layer of functional endodermis, as is predicted by Cui et al. (4). It is possible that some of the ground tissue layers in the roots expressing the SHR homologs or AtSHR had mixed cell identity, with partial endodermal and cortex cell character. However, the PI exclusion assays and lignin autofluorescence indicate that while SHR is necessary for specification of a functional endodermis, it is not sufficient.

A major feature of the ground tissue patterning model proposed by Cui et al. (4) was the ability of SCR to inhibit SHR movement via direct protein–protein interaction and sequestration in the nuclei of endodermal cells. While we cannot entirely rule out differences in the levels of SCR expression between the roots expressing the *A. thaliana* and grass SHR proteins, our results suggest that the direct binding of AtSCR to the monocot SHR proteins is insufficient to inhibit movement from the endodermis. SCR is, however, responsible for the nuclear localization of OsSHR1, OsSHR2, and BdSHR. To minimize the apparent differences between the behaviors of the SHR

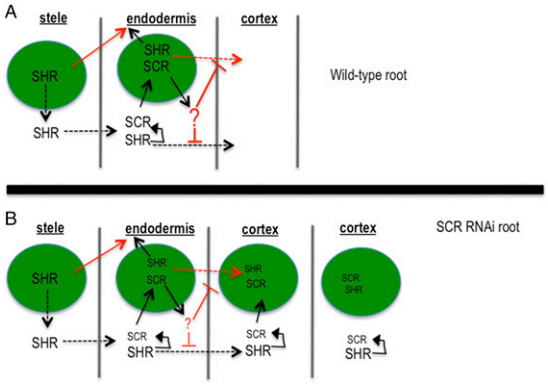

Fig. 6. Revised model for ground tissue patterning (4). The green circles are nuclei. Dotted lines indicate protein movement. The size of the font is meant to indicate the relative amount of the protein. (*A*) The pathways for the formation of a wild-type *A. thaliana* root and (*B*) one in which SCR is reduced via RNA interference. The arrows and text shown in red are modifications to the previous model. Unlike the previous model proposed by Cui et al. (4), SCR-dependent nuclear localization and restriction of SHR movement are separable. The ability of the monocot SHR proteins to interact with SCR and localize to nuclei, yet move past the endodermis, indicates that a factor downstream of SCR (indicated by "?") is important for inhibiting movement of AtSHR.

proteins, we propose a modified model for the regulation of SHR movement, in which SCR directly promotes the nuclear localization of AtSHR (along with the SHR homologs) and indirectly blocks movement through the up-regulation of an unidentified factor, indicated by "?" in Fig. 6, that inhibits movement of AtSHR from the endodermis. This revised model is based upon several lines of evidence. First, all of the SHR homologs can bind to AtSCR and all of the SHR homologs are nuclear localized in the ground tissue, yet they move beyond the endodermis in both *shr-2* and in wild-type roots. These results indicate that neither nuclear localization of SHR in the ground tissue nor binding of SHR to SCR is sufficient to block intercellular movement. In addition, previous results showed that the inclusion of a nuclear export signal in AtSHR-GFP caused cytoplasmic localization of AtSHR-GFP in the endodermis, yet the protein was restricted to the endodermis, presumably due to the presence of an SCR-dependent factor that prevents movement of AtSHR, independent of nuclear localization (21). Likewise, Sena et al. showed that when expressed in the epidermis of wild-type roots (where SCR is not normally expressed), AtSHR showed little movement into the cortex; however in the *scr* mutant background, AtSHR moved freely into the cortex (20). All of these data point to the presence of a SCR-dependent factor that restricts movement of AtSHR (but not OsSHR1, OsSHR2, or BdSHR) in the endodermis. This is in contrast to the original model in which the direct binding of AtSHR by SCR resulted in the nuclear localization of AtSHR, resulting in restricted movement (4).

A conserved mechanism limiting the movement of SHR is used to explain the formation of one endodermal cell layer in plant roots (Fig. 1) (4). This hypothesis was based, in part, upon previous data showing that ectopic expression of AtSHR can change the properties of the cell wall and induce production of suberin, which was used as a marker of endodermis. For example, in Nakajima et al. (7), expression of SHR from the SCR promoter caused the formation of supernumerary ground tissue layers that produced suberin. Recently, work by Naseer et al. has questioned the usefulness of suberin as a marker of endodermis; instead, they have shown that a functional endodermis is lignified and able to exclude PI in the absence of suberin (18). Here we show, using the EN7-HC, CO_2-HC, and PIN2-GFP markers (14, 16), as well as lignin autofluorescence and PI exclusion assays, that the expression of the SHR homologs in *A. thaliana* roots results in the formation of a single endodermal cell layer and multiple layers of cortex. In addition, reexamination of the lines that show either ectopic movement or ectopic expression of AtSHR indicates that AtSHR also has a limited ability to specify functional endodermis, even with the production of suberin.

All of our data are consistent with the SHR proteins having a spatially restricted ability to specify endodermis that is independent of the extent of protein movement. Because it is the SHR-containing ground tissue layer in contact with the stele that develops as endodermis, it may be a stele-derived signal that participates with SHR to induce endodermal specification. It is this signal that is the critical factor in the formation of a single endodermal cell layer next to the stele. In the context of the monocot roots, the spatial restriction of the stele-derived signal in the presence of increased movement of SHR represents a plausible and testable mechanism for the formation of multiple layers of cortex without an expansion of the endodermis. In this context, the regulation of the extent of SHR movement would control the number cortex cell layers, which in rice and *B. distachyon* differs between root segments on the same plant.

Materials and Methods

All plants were grown on 1% agar plates with 0.5x Murashige and Skoog (MS) medium under a 16-h light/8-h dark cycle at 23 °C. Five- to six-day-old plants were used for all experiments unless otherwise stated. Roots were counterstained in 0.01 μg/mL PI in water. Confocal images were obtained using a 20× water-immersion lens on a Leica TCS SL microscope. The yeast two-hybrid assays were tested in diploid yeast cells by mating the two yeast strains, Y187 and AH109. BiFC assays were performed in protoplasts extracted from *A. thaliana*. Details are provided in *SI Materials and Methods*.

ACKNOWLEDGMENTS. J. Ugochukwu and C. Heyworth provided technical support. D. Wagner provided comments on the manuscript. A. Stout manages the confocal facility. S.W. and C.-M.L. are partially supported by National Science Foundation Grant 1243945 awarded to K.L.G.

1. Dolan L, et al. (1993) Cellular organisation of the *Arabidopsis thaliana* root. *Development* 119(1):71–84.
2. Clark LH, Harris WH (1981) Observations on the root anatomy of rice (*Oryza-Sativa*-L). *Am J Bot* 68(2):154–161.
3. Watt M, Schneebeli K, Dong P, Wilson IW (2009) The shoot and root growth of *Brachypodium* and its potential as a model for wheat and other cereal crops. *Funct Plant Biol* 36(11):960–969.
4. Cui H, et al. (2007) An evolutionarily conserved mechanism delimiting SHR movement defines a single layer of endodermis in plants. *Science* 316(5823):421–425.
5. Gallagher KL, Paquette AJ, Nakajima K, Benfey PN (2004) Mechanisms regulating SHORT-ROOT intercellular movement. *Curr Biol* 14(20):1847–1851.
6. Helariutta Y, et al. (2000) The SHORT-ROOT gene controls radial patterning of the *Arabidopsis* root through radial signaling. *Cell* 101(5):555–567.
7. Nakajima K, Sena G, Nawy T, Benfey PN (2001) Intercellular movement of the putative transcription factor SHR in root patterning. *Nature* 413(6853):307–311.
8. Sozzani R, et al. (2010) Spatiotemporal regulation of cell-cycle genes by SHORTROOT links patterning and growth. *Nature* 466(7302):128–132.
9. Welch D, et al. (2007) *Arabidopsis* JACKDAW and MAGPIE zinc finger proteins delimit asymmetric cell division and stabilize tissue boundaries by restricting SHORT-ROOT action. *Genes Dev* 21(17):2196–2204.
10. Vatén A, et al. (2011) Callose biosynthesis regulates symplastic trafficking during root development. *Dev Cell* 21(6):1144–1155.
11. Paquette AJ, Benfey PN (2005) Maturation of the ground tissue of the root is regulated by gibberellin and SCARECROW and requires SHORT-ROOT. *Plant Physiol* 138(2): 636–640.
12. Koizumi K, Hayashi T, Gallagher KL (2012) SCARECROW reinforces SHORT-ROOT signaling and inhibits periclinal cell divisions in the ground tissue by maintaining SHR at high levels in the endodermis. *Plant Signal Behav* 7(12):1573–1577.
13. Koizumi K, Wu S, MacRae-Crerar A, Gallagher KL (2011) An essential protein that interacts with endosomes and promotes movement of the SHORT-ROOT transcription factor. *Curr Biol* 21(18):1559–1564.
14. Koizumi K, Gallagher KL (2012) Identification of SHRUBBY, a SHORT-ROOT and SCARECROW interacting protein that controls root growth and patterning. *Development* (140):1292–1300.
15. Koizumi K, Hayashi T, Wu S, Gallagher KL (2012) The SHORT-ROOT protein acts as a mobile, dose-dependent signal in patterning the ground tissue. *Proc Natl Acad Sci USA* 109(32):13010–13015.
16. Heidstra R, Welch D, Scheres B (2004) Mosaic analyses using marked activation and deletion clones dissect *Arabidopsis* SCARECROW action in asymmetric cell division. *Genes Dev* 18(16):1964–1969.
17. Blilou I, et al. (2005) The PIN auxin efflux facilitator network controls growth and patterning in *Arabidopsis* roots. *Nature* 433(7021):39–44.
18. Naseer S, et al. (2012) Casparian strip diffusion barrier in *Arabidopsis* is made of a lignin polymer without suberin. *Proc Natl Acad Sci USA* 109(25):10101–10106.
19. Geldner N (2013) The endodermis. *Annu Rev Plant Biol* 64:531–558.
20. Sena G, Jung JW, Benfey PN (2004) A broad competence to respond to SHORT ROOT revealed by tissue-specific ectopic expression. *Development* 131(12):2817–2826.
21. Gallagher KL, Benfey PN (2009) Both the conserved GRAS domain and nuclear localization are required for SHORT-ROOT movement. *Plant J* 57(5):785–797.

Supporting Information

Wu et al. 10.1073/pnas.1407371111

SI Materials and Methods

Plasmid Construction and Plant Transformation. The full-length cDNA of OsSHR1 and OsSHR2 were PCR amplified from Nipponbare genomic DNA using KOD taq from Invitrogen. PCR products were first cloned into the pCR-XL-TOPO vector (TOPO XL Cloning Kit, Invitrogen). From there, the OsSHR1 and OsSHR2 clones were reamplified to add recombination sites for insertion into pDONR221 (Invitrogen). BdSHR was cloned directly from genomic DNA and recombined into pDONR221. The mutant form of the SHR homologs were generated using inverse PCR. After sequencing, the resulting plasmids were all recombined into Gateway destination vectors. To achieve cell-specific expression, the previously reported pGreenBarT vector (1) was modified. The attR4/R3 gateway cassettes were replaced by attR1/R2 cassettes flanked by two multiple cloning sites. The promoter sequence of SHR was amplified and cut by Kpn1/Xho1, and pEN7 and pCO2 sequences were amplified and cut by KpnI/KpnI. The digested fragments were ligated into the multiple cloning sites 5′ of the gateway cassette using corresponding restriction sites. YFP and mCherry sequence were cloned and digested by XbaI and HindIII before insertion into the multiple cloning sites 3′ of the gateway cassette. The BiFC plasmid were prepared by amplification of the 35S:Venus-Gateway-NosT cassette from pDEST-VYCE(R)GW or pDESTVYNE(R)GW vectors (2) and subcloned into SmaI site in the pUC18 vector.

All resulting plasmids generated through LR Gateway reaction were transformed into Agrobacterium strain GV3101-pSoup-pMP. The Agrobacterium was then used to transform *Arabidopsis* (Col-0) following the floral dip method (3). Transgenic plants were screened by using resistance to glufosinate-ammonium (Basta) in soil. For all of the transgenes discussed, at least three independently transformed lines were analyzed.

Plant Materials and Growth Condition. *Arabidopsis thaliana* Columbia line (Col-0) was used as the wild type throughout the experiments. Plants were germinated and grown vertically on 0.5x MS medium (Caisson) containing 0.05% (wt/vol) Mes (pH5.7), 1.0% (wt/vol) Sucrose, and 1% Granulated agar (DIFCO) in a growth chamber at 23 °C under a 16-h light/8-h dark cycle. Plants were imaged 5–6 d after plating unless otherwise stated. After sterilization, the *B. distachyon* seeds were germinated in darkness on wet filter papers placed in a Petri dish. The roots of 1-wk-old seedlings were then collected for anatomy analysis. For cross sections, the rice seeds were sterilized by 70% ethanol for 1 min, followed by bleach (20/30, vol/vol) for 30 min. After three washes in distilled sterile water, the rice seeds were germinated on 0.5x MS media and grown vertically in a Petri plate (20 × 20 cm, Corning) for 6 d (10 h light/12 h dark at 24/26 °C). The SHR homolog lines in different genetic backgrounds were obtained by crossing. The progeny was followed to the second generation, and the presence of transgene or mutation was verified either by imaging on the confocal or genotyping.

Confocal Microscopy. Roots were counterstained in 0.01 μg/mL propidium iodide (PI) in water. Confocal images were obtained using a 20× water-immersion lens on a Leica TCS SL microscope equipped with an argon–krypton ion laser with the appropriate filter sets for visualizing YFP and PI. The dual-channel observation of YFP and mCherry was conducted on a Zeiss LSM 710 laser scanning confocal microscope using a Zeiss LD C-Apochromat 40×/1.1 NA water immersion objective lens (Carl Zeiss Microimaging, Inc.).

BiFC Assay in *Arabidopsis* Protoplast. Protoplasts were isolated from 3-wk-old plants grown under normal light conditions with tape-*Arabidopsis* sandwich method (4) and enzyme solution containing 1.5% (wt/vol) Cellulase R-10 and 0.5% Macerozyme R-10 (Yakult Pharmaceutical). The transfection was conducted as described by ref. 5. Briefly, the mixture of 10 μg of freshly isolated plasmid DNA and an equal volume of a solution of 40% (vol/vol) PEG (MW 4000; Fluka) with 0.1 M CaCl2 and 0.2 M mannitol was incubated at room temperature for 13 min and then washed in W5 solution (154 mM NaCl, 125 mM CaCl2, 5 mM KCl, 5 mM glucose, and 2 mM Mes, pH 5.7). After 16–24 h incubation in low-light conditions, protoplasts were imaged on a Leica TCS SL microscope using a 20× water-immersion lens. The Venus emission was captured using a 510- to 540-nm filter. To quantify the interactions between AtSCR and SHR homologs, the Venus signals in the nuclei were selected and the mean intensities were measured using ImageJ. Quantification was done as referenced in refs. 6 and 7.

Histology and Histochemistry. The seedlings were fixed for 1 h in formalin–acetic acid–alcohol and then embedded in an agarose block as described previously (8). The agarose blocks containing samples were dehydrated in a graded series of 50%, 70%, 90%, and 2 × 100% (vol/vol) ethanol. Technovit 7100 (EMS; no. 14653) infiltration was performed according to the manufacturer. Then, 3- to 5-μm sections were made on a Leitz 1512 rotary microtome using Thermo HP 35 steel blades. Sections were stained in fresh 0.01% toluidine blue-O (Merck). *B. distachyon* roots were fixed, dehydrated, and embedded in the same manner as *Arabidopsis* except omitting the agarose embedment step. To obtain cross-sections of rice roots, the tip of rice roots (~1 cm) were collected and embedded in a 3% agarose block. Around 50-μm sections were then performed on a Microtome HM 650 V vibratome. Images of cross-sections of *A. thaliana* and *B. distachyon* were captured by an Olympus BX51 microscope equipped with a digital camera. The cross-sections of rice roots were photographed under UV light using a DAPI filter on a Leica DMX6000 microscope.

PI Exclusion and Autofluorescence of Casparian Strips. For assay of the functional endodermis, seedlings were incubated for 10 min in a freshly made PI solution of (10 μg/mL) and then rinsed twice in distilled water before confocal imaging.

To detect the autofluorescence of Casparian strips, roots were transferred to a 12-well plate containing 0.24 N HCl in 20% (vol/vol) methanol and incubated at 57 °C for 15 min. Roots were then treated with 7% (wt/vol) NaOH in 60% (vol/vol) ethonal for 15 min at room temperature. After rehydration in a graded series of 40%, 20%, and 10% (vol/vol) ethanol for 5 min each, roots were infiltrated in 5% (vol/vol) ethanol and 25% (vol/vol) glycerol for 15 min. Roots were then mounted in 50% (vol/vol) glycerol and observed on an Olympus BX51 microscope with a GFP filter.

Estrogen Induction. Five days after plating, the seedlings were transferred to 0.5x MS (Caisson) agar (Difco-BBL) plates containing 10 μM estradiol (Sigma), and the same medium containing the estradiol carrier (ethanol) as controls. The seedlings were returned to the growth chamber and incubated vertically for 1 d before confocal imaging.

FRAP. The FRAP assay was performed as described before (9). Briefly, photobleaching of GFP signal in endodermis was

achieved using six iterations of the 488-nm laser at 100% power on a Leica TCS SL microscope equipped with an argon–krypton ion laser. Recovery was followed by image acquisition using 20% laser power at 30-min intervals. The seedlings were placed in the moisture box during the intervals. Nine roots from three experiments and 35–132 cells for SHR homolog were analyzed. The fluorescence intensity ratio (endodermis/stele) before bleach, after bleach, and after recovery was determined using ImageJ. The percent recovery was calculated using the normalized values as described previously (9).

Yeast Two-Hybrid Assay. The coding sequences of AtSHR, OsSHR1, OsSHR2, AtSCR, AtMGP, and AtJDW were cloned into pDEST22 or pDEST32 vectors (Invitrogen) as bait or prey constructs and transformed into the yeast strain Y187 and AH109, respectively. The protein–protein interactions were tested in diploid yeast cells by mating the two yeast strains as described by the Matchmaker protocol (Clontech).

For β-galactosidase assays, yeast cultures were grown in selective medium to an optical density at 595 nm (OD595) of 0.8 to 1, and the β-galactosidase assays were performed as described previously (10). The specific activities were determined by the β-galactosidase enzymatic activity normalized to the concentration of crude protein from three independent biological replicates.

1. Lee JY, et al. (2006) Transcriptional and posttranscriptional regulation of transcription factor expression in *Arabidopsis* roots. *Proc Natl Acad Sci USA* 103(15): 6055–6060.
2. Gehl C, Waadt R, Kudla J, Mendel RR, Hänsch R (2009) New GATEWAY vectors for high throughput analyses of protein-protein interactions by bimolecular fluorescence complementation. *Mol Plant* 2(5):1051–1058.
3. Clough SJ, Bent AF (1998) Floral dip: A simplified method for Agrobacterium-mediated transformation of *Arabidopsis thaliana*. *Plant J* 16(6):735–743.
4. Wu FH, et al. (2009) Tape-*Arabidopsis* Sandwich - A simpler *Arabidopsis* protoplast isolation method. *Plant Methods* 5:16.
5. Yoo SD, Cho YH, Sheen J (2007) *Arabidopsis* mesophyll protoplasts: A versatile cell system for transient gene expression analysis. *Nat Protoc* 2(7):1565–1572.
6. Rose RH, Briddon SJ, Holliday ND (2010) Bimolecular fluorescence complementation: Lighting up seven transmembrane domain receptor signalling networks. *Br J Pharmacol* 159(4):738–750.
7. Sung MK, et al. (2013) Genome-wide bimolecular fluorescence complementation analysis of SUMO interactome in yeast. *Genome Res* 23(4):736–746.
8. Wu S, Baskin TI, Gallagher KL (2012) Mechanical fixation techniques for processing and orienting delicate samples, such as the root of *Arabidopsis thaliana*, for light or electron microscopy. *Nat Protoc* 7(6):1113–1124.
9. Wu S, Gallagher KL (2013) Intact microtubules are required for the intercellular movement of the SHORT-ROOT transcription factor. *Plant J* 74(1):148–159.
10. Guarente L (1983) Yeast promoters and lacZ fusions designed to study expression of cloned genes in yeast. *Methods Enzymol* 101:181–191.

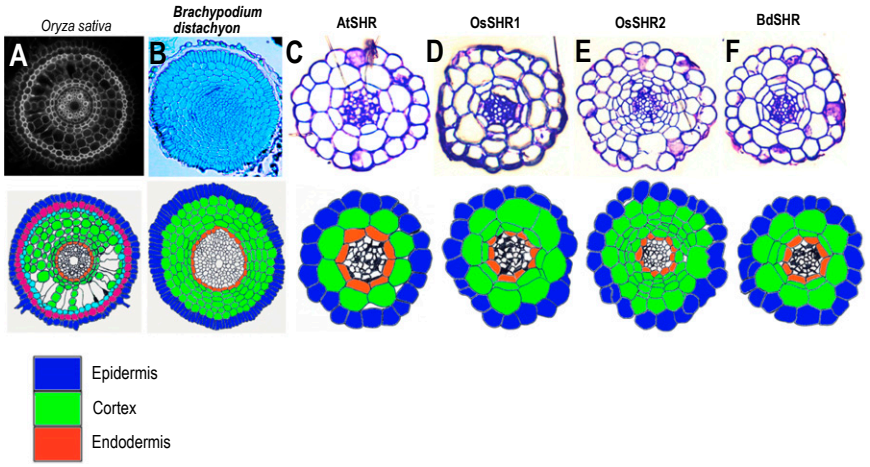

Fig. S1. Root anatomy. (*A*–*C*) Transverse cross-section through the roots of *O. sativa*, *B. distachyon* and *A. thaliana* as indicated. (*D*–*F*) Transverse cross-section through roots of *A. thaliana* expressing the indicated transgenes. Below each root image is a cartoon tracing of the root that has been color coded to indicate the identity of the cell layers.

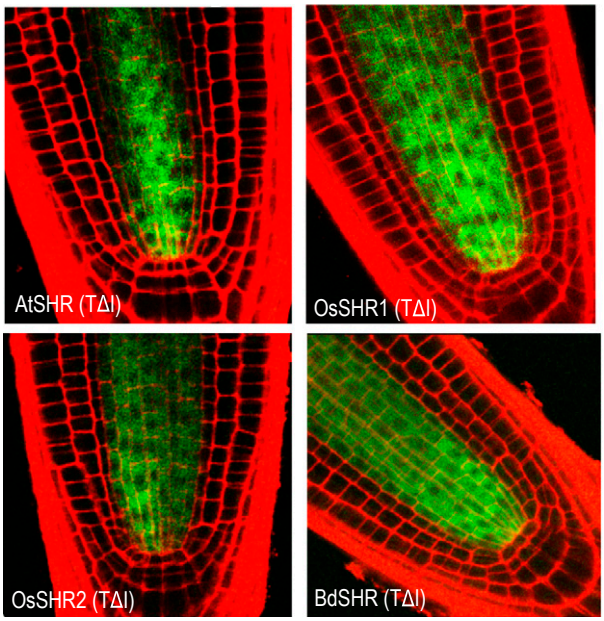

Fig. S2. Full root tip confocal images of the cropped images shown in Fig. 2*A*. All roots express a mutated version of SHR (as labeled) that converts a conserved threonine in the VHIID domain into an isoleucine.

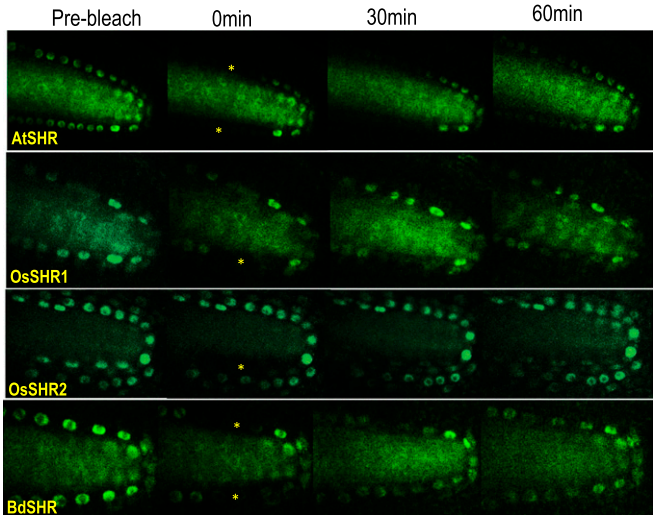

Fig. S3. The monocot SHR proteins recover movement within a similar time frame as AtSHR. Fluorescence recovery after photobleaching (FRAP) of the SHR-YFP signals in the first ground tissue layer was monitored for 60 min. The yellow asterisks mark the cell layers that were photobleached.

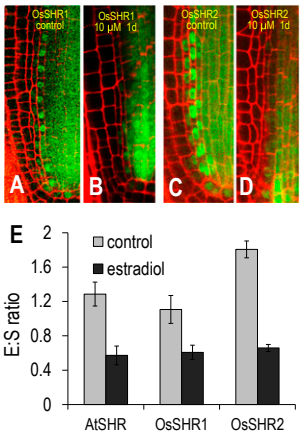

Fig. S4. The monocot SHR proteins move via plasmodesmata (PD). (*A*–*D*) Expression of the icals3m transgene from the WOODENLEG (WOL) promoter blocks PD and movement of the indicated SHR proteins. (*E*) Quantification of the fluorescence ratio (endodermis against stele, E:S) after induction of WOL:icals3m (2, 3).

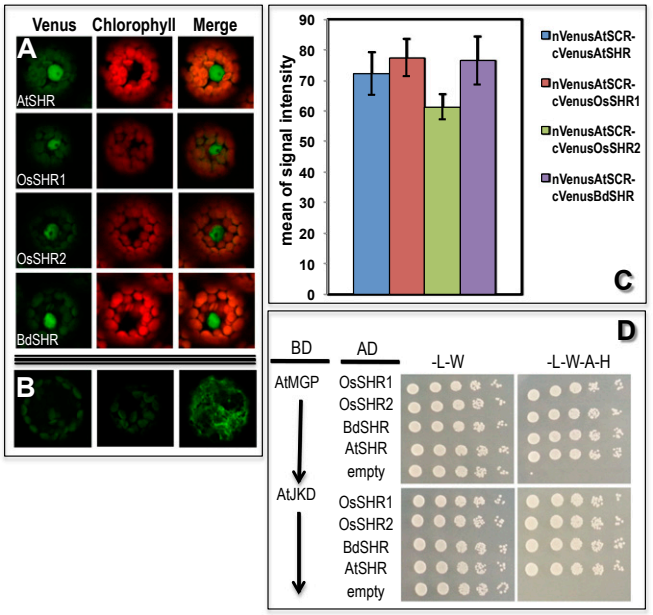

Fig. S5. The interactions of AtSCR and SHR homologs in *Arabidopsis* leaf protoplasts. (*A*) Representative confocal images show BiFC between AtSCR and the SHR homologs in *A. thaliana*, *O. sativa*, and *B. distachyon*. Shown are images of (*Left*) Venus (BiFC), (*Middle*) autofluorescence from chlorophyll, and (*Right*) the overlay. (*B*) Representative images of BiFC controls: (*Left*) empty vectors and (*Middle* and *Right*) representative images of the empty n-Venus vector transfected with SHR c-Venus plasmid. The nonspecific cytoplasmic fluorescence shown in *Right* was absent in the assays using AtSCR n-Venus with the SHR c-Venus constructs. (*C*) Quantitation of BiFC as detailed in *SI Materials and Methods*. Results indicate that the strength of interaction between AtSCR and the SHR homologs from *O. sativa* and *B. distachyon* are not significantly different from the interaction between AtSCR and AtSHR. Each bar represents the average fluorescent intensity in nuclei from 22 to 25 protoplasts. (*D*) Fivefold serial dilutions of diploid yeast expressing AtMGP or AtJKD as bait with the SHR prey proteins (as labeled) growing on selective medium. Medium lacking adenine and histidine are used to select for interaction between the bait and prey proteins. AD, activation domain vector (prey). BD, binding domain vector (bait).

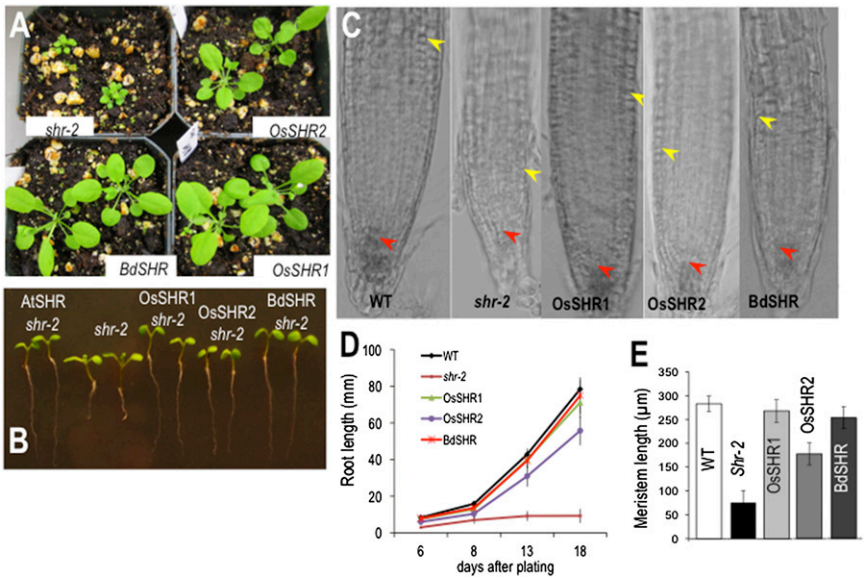

Fig. S6. Complementation of *shr-2* mutants with the SHR homologs. (*A*) Four-week-old *shr-2* seedlings without and with the SHR transgenes as indicated. (*B*) One-week-old *shr-2* seedlings without and with the SHR transgenes as indicated. (*C*) Differential interference contrast (DIC) images of the root meristems of the 6-d-old *shr-2* seedlings and *shr-2* without and with the SHR transgenes as indicated. Red arrowheads point to the QC, and yellow arrowheads mark the initial expansion site in the root. (*D*) Comparison between the growth of the *shr-2* roots without and with the SHR transgenes as indicated at 3, 5, 10, and 15 d after germination ($n = 3$ replicates, 36 roots for each line). Meristem length was defined as the distance between the QC and the first expanded cell in the cortex and is indicated in *E*. Only OsSHR2 and shr-2 are statistically different from wild type (*t* test, $P < 0.005$) ($n = 3$ replicates, 24 roots for each line).

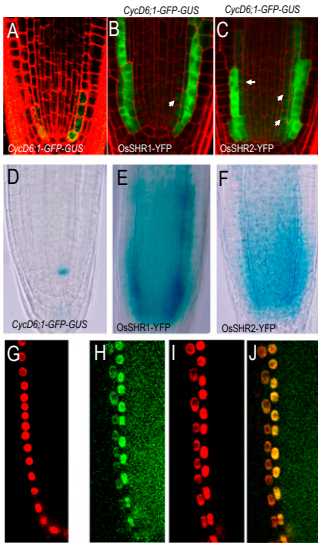

Fig. S7. Expression of *CYCD6;1:GUS-GFP* and SCR-mCherry. (*A*–*C*) Confocal sections through the root meristem showing both the expression of *GUS-GFP* and the SHR-YFP proteins from the CYCD6 ;1 and SHR promoters, respectively. Arrows point to the OsSHR-YFP fluorescence in endodermis. (*D*–*F*) β-Glucuronidase (GUS) staining of the roots without (*D*) and with the SHR transgenes (as indicated). (*G*–*I*) Expression of pSCR:SCR-mCherry in (*G*) wild-type and (*I*) a root expressing OsSHR1 from the SHR promoter. The image in *H* is OsSHR1-YFP, and *J* shows the overlay between *H* and *I*.

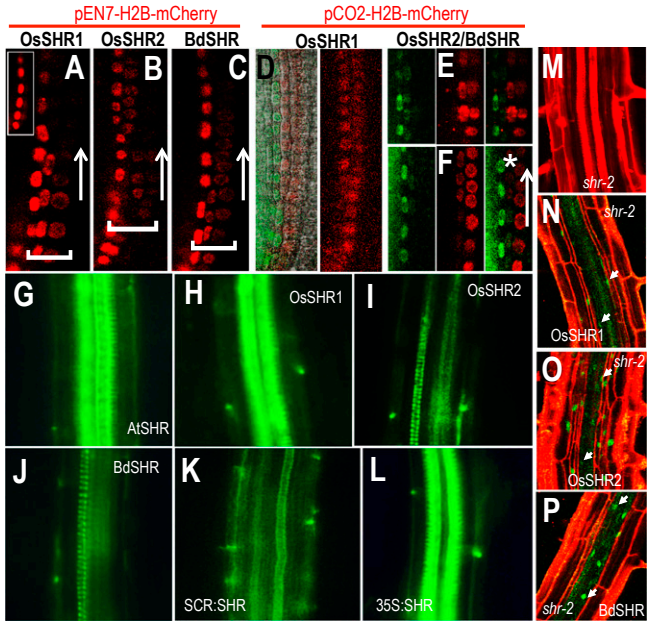

Fig. S8. All roots examined have a single layer of endodermis. (*A*–*C*) Expression of pEN7-HC in the root expressing SHR proteins as labeled. The arrows point shootward. (*D*–*F*) Expression of pCO2-HC in roots expressing the SHR proteins as labeled. The arrows point shootward. The white asterisk marks the cortex cell layer. (*G*–*L*) Lignified Casparian strips visible as green autofluorescence of cell walls (marked by the white arrows). (*M*–*P*) PI staining in *shr-2* roots expressing the SHR proteins as labeled. White arrows point to the nuclear localization of SHR in the endodermis.